State changing in collisions of Rb(ns) Rydberg atoms with HF

A. Kalamarides, L. N. Goeller, K. A. Smith, F. B. Dunning, M. Kimura,* and N. F. Lane
Department of Space Physics and Astronomy, Department of Physics, and the Rice Quantum Institute, Rice University, P.O. Box 1892, Houston, Texas 77251
(Received 10 November 1986; revised manuscript received 15 May 1987)

Rate constants for state changing in collisions of Rb(ns) Rydberg atoms ($40 \leqq n \leqq 48$) with HF molecules have been measured and have been calculated using a semiclassical approach. Agreement between the total rate constants measured experimentally and derived theoretically is very good. The results point to the near-resonant nature of n-changing collisions, but indicate that the rate constants for such reactions are less dependent on energy imbalance than suggested by calculations based on the impulse approximation.

Recent investigations have shown that collisions between atoms in Rydberg states and polar molecules can lead to ionization and to changes in the quantum states of the excited atoms.[1-5] In the present work we have investigated the state-changing reactions

$$\mathrm{Rb}(ns)+\mathrm{HF}(J)\rightarrow\mathrm{Rb}(n',l')+\mathrm{HF}(J)\ , \quad (1)$$

$$\mathrm{Rb}(ns)+\mathrm{HF}(J=1)\rightarrow\mathrm{Rb}(n'',l'')+\mathrm{HF}(J=0)\ , \quad (2)$$

$$\mathrm{Rb}(ns)+\mathrm{HF}(J=0)\rightarrow\mathrm{Rb}(n''',l''')+\mathrm{HF}(J=1)\ , \quad (3)$$

for Rb(ns) atoms with values of principal number n in the range from 40 to 48. Absolute rate constants for these reactions, and for total depopulation of the parent ns states, are reported together with the results of theoretical calculations undertaken using a semiclassical model in which the atom and molecule are represented quantum mechanically, but their relative motion is described classically. The agreement between theory and experiment is very good. The data again point to the near-resonant nature of n-changing collisions, i.e., reactions (2) and (3), which involve an interchange of molecular rotational energy and energy of electronic excitation. The rate constants for such reactions are expected to depend on the energy imbalance ΔE, i.e., the difference between the rotational energy gained (lost) by the polar molecule and the electronic energy lost (gained) by the excited atom. The present experimental and theoretical results indicate, however, that the reaction rates are less critically dependent on the energy imbalance than suggested by quantum-mechanical impulse-approximation calculations.[5,6]

The present apparatus and experimental technique have been described in detail elsewhere.[7] Briefly, rubidium atoms contained in a thermal-energy beam are excited to a selected ns state by two-photon excitation using a Coherent Radiation model 699-21 frequency-stabilized single-mode Rh6G ring dye laser. The laser output is modulated by a fast Pockels cell to provide light pulses of 1 μsec duration at a repetition frequency of $\sim 10-20$ kHz. Excitation occurs, in zero electric field and (typically) in the presence of target gas, near the center of an interaction region defined by two planar, parallel fine-mesh grids. Following excitation, collisions are allowed to occur for a selected time interval t, typically $\sim 4-16$ μsec, whereupon the excited-state distribution of the atoms present in the interaction region is determined by selective field ionization (SFI).[1-3,8] In SFI a pulsed electric field, which rises from zero to ~ 1400 V cm^{-1} in 1 μsec, is applied in the interaction region. The electrons liberated by ionization are accelerated to a particle multiplier whose output is fed to a time-to-digital converter (TDC). The TDC is started at the beginning of the ionizing ramp and is stopped by the first subsequent output pulse from the multiplier. The output from the TDC is fed to an LSI 11/23 minicomputer that operates as a multichannel analyzer. For the present signal count rates, typically ~ 100 Hz, the data stored in the computer give the probability of a field ionization event per unit time during the ionizing ramp. Measurement of the time dependence of the ionizing field strength then permits the field dependence of the ionization signal to be determined. Because Rydberg atoms in different quantum states ionize at different field strengths, analysis of the resultant SFI profiles permits discrimination of the products of reactions (1)–(3) from each other and from remaining parent ns atoms.

A given SFI feature can only be correlated with a particular initial zero-field Rydberg state if the nature of the path to ionization is known. Earlier investigations have shown that, in an increasing electric field, Rydberg atoms typically follow either predominantly adiabatic or predominantly diabatic paths to ionization and that, for a particular initial value of n, these paths lead to ionization at substantially different electric field strengths. The probability of diabatic ionization increases both with n and $|m_l|$. For the values of n of interest here, Rb(nl) states having $|m_l| \leq 2$ tend to follow adiabatic paths to ionization whereas those with $|m_l| > 2$ tend to field ionize diabatically.

A typical SFI profile obtained in the absence of target gas 16 μsec after excitation of Rb(42s) atoms is shown in

Fig. 1(b). Figure 1(a) shows the SFI profile obtained, at the same time delay, following excitation in the presence of target gas. Several new SFI features resulting from ionization of states populated by collisions are evident, and these are more clearly apparent in Fig. 1(c) which shows the difference between the gas-in and gas-out SFI profiles. As an aid to interpreting the various SFI features, a series of bars are shown beneath the data to indicate the range of field strengths over which states populated through reactions (1)–(3) are expected to ionize. The large central peaks in both Figs. 1(a) and 1(b) result predominantly from adiabatic ionization of atoms in the parent 42s state. The other small features evident in Fig. 1(b) arise from ionization of states populated through blackbody-radiation-induced transitions.[9] The features P_2 result from adiabatic and diabatic ionization of atoms in states with $n \sim 59$ that are produced via reaction (2). The P_2 features are well resolved indicating that reaction (2) must be near resonant and result in the production of only a limited range of final n states. The relative sizes of the P_2 peaks suggest that the majority of the product atoms is in states that ionize diabatically, i.e., states of high $|m_l|$. The relative sizes of the two P_2 features are consistent with that expected for ionization of atoms having a near statistical distribution of l values. The feature P_1 results predominantly from diabatic ionization of states in the $n=39$ manifold (which, because of the large quantum defect associated with Rb(ns) states, is the manifold of high-l states lying closest in energy of the parent 42s level) populated through reaction (1). Adiabatically ionizing low-$|m_l|$ products of reaction (1) are obscured by the large feature associated with ionization of parent 42s atoms. P_3 results from diabatic ionization of states with $n \sim 31$ produced through reaction (3). The small shoulder evident on the high-field side of P_1 may be associated with products of this reaction that ionize adiabatically, but the data again suggest that the majority of the collision products is in high-l states.

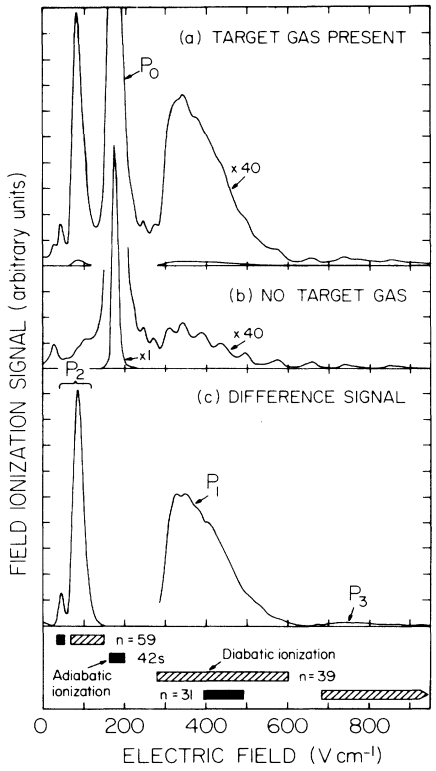

FIG. 1. (a) SFI profile obtained with HF target gas present in the interaction region. (b) SFI profile obtained in the absence of target gas. (c) SFI signal due to ionization of states populated through collisions. The horizontal bars beneath the data indicate the ranges of electric field strength over which adiabatic and diabatic ionization of states populated through reactions (1)–(3) is expected.

Rate constants for reactions (1)–(3), and for total depopulation of the parent state, are derived from measurements of the time dependence of the populations in the appropriate SFI features, which are corrected for background signals due to blackbody-radiation-induced effects. Rate constants k_d for total collisional depopulation are determined from the time development of the ns population, i.e., P_0. If $N(0)$ ns Rydberg atoms are initially excited, then at any later time t the number remaining is given by

$$N(t)=N(0)\exp\left[-\left[\frac{1}{\tau_{\text{eff}}}+\rho k_d\right]t\right], \tag{4}$$

where τ_{eff} is the effective lifetime of the parent state, determined by measurements of $N(t)$ in the absence of target gas, and ρ is the total target-gas density. ρ is measured by an ionization gauge calibrated against a capacitance manometer. Measurements showed that, over the pressure range from 5×10^{-5} to 4×10^{-4} torr, the pressure indicated by the ion gauge was directly proportional to the absolute pressure as recorded by the capacitance manometer. It is thus reasonable to assume that the same ion-gauge sensitivity applies at the lower pressures ($\sim10^{-6}$ torr) employed in the present collision studies. Values of $N(t)$ are typically obtained at four separate times t, and k_d is determined from a fit of Eq. (4) to the data.

To obtain rate constants for reaction (1) the collision products are treated as a reservoir of population, say, $R(t)$. A small correction is applied in determining $R(t)$ to account for the fact that the feature P_1 results only from the diabatically ionizing products of reaction (1). In deriving this correction, it is assumed that the states comprising the reservoir have a statistical distribution of l values. Ignoring multiple collisions, the time development of the reservoir population is described by the rate equation

$$\frac{dR(t)}{dt}=\rho k N(t)-R(t)/\tau_{R,\text{eff}}, \tag{5}$$

where k is the rate constant for reaction (1) and $\tau_{R,\text{eff}}$ is the effective lifetime of the atoms comprising the reservoir. The integral form of Eq. (5) is fitted to the observed time development of the reservoir population, thereby obtaining the rate constant k. A similar approach is adopted to obtain the rate constants for reac-

tions (2) and (3). However, whereas all the target molecules can contribute to collisional depopulation and to reaction (1), only those with $J=1$ and 0 participate in reactions (2) and (3), respectively. The density ρ appearing in Eq. (5) must therefore be modified to reflect that, at 300 K, only $\sim 10\%$ of the target atoms are in the $J=0$ rotational state and only $\sim 24\%$ are in the $J=1$ state.

Measured rate constants for total collisional depopulation and for reaction (1) are presented in Fig. 2. Data for n changing, i.e., reactions (2) and (3), are shown in Fig. 3. These data can be used to derive rate constants for collisional ionization via the reaction

$$\mathrm{Rb}(ns)+\mathrm{HF}(J\geq 2)\rightarrow \mathrm{Rb}^{+}+e^{-}+\mathrm{HF}(J-1) \qquad (6)$$

by assuming that collisional depopulation of parent atoms results only from reactions (1)–(3) and (6). The rate constants determined in this manner for reaction (6) are $\sim 6\times 10^{-7}\ \mathrm{cm}^3\,\mathrm{sec}^{-1}$ and are essentially independent of n over the present range.

Rate constants for state-changing collisions calculated using the impulse approximation[6,10] and the present semiclassical[11] theory are also contained in Figs. 2 and 3. In the semiclassical theory the relative motion of the heavy particles, i.e., the atomic-core ion and center of mass of the molecule, is treated classically. Because earlier classical studies[12] demonstrate that all the processes of interest here are dominated by Rydberg electron-molecule interactions and hence by large impact parameters, this motion is taken to be rectilinear. Since it is reasonable to expect that a large number of nearly degenerate Rydberg states will be strongly mixed by the field of the polar molecule during the collision, a close-coupling expansion is employed. For each impact parameter describing the heavy-particle motion the time-dependent wave function describing the internal (Rydberg electron plus molecular rotation) motion is expanded in the form

$$\Psi(\mathbf{r},\hat{\xi},t)=\sum_i a_i(t)\phi_i^{\mathrm{AO}}(\mathbf{r})\chi_i^{\mathrm{PRM}}(\hat{\xi};\mathbf{r})\ , \qquad (7)$$

where $\phi_i^{\mathrm{AO}}(\mathbf{r})$ is a Rydberg atomic orbital (AO) in terms of electron coordinates $\mathbf{r}$, and $\chi_i^{\mathrm{PRM}}(\hat{\xi};\mathbf{r})$ is an eigenfunction, in terms of rotational coordinates $\hat{\xi}$, of the "perturbed rotating molecule" (PRM) Hamiltonian, i.e., the Hamiltonian for the rotating molecule perturbed by the field of the electron. The Rydberg atomic orbitals are approximated by a Slater-type orbital (STO) adjusted by the quantum defect of the state. Although the STO is a good approximation to the hydrogenic radial function only in the regions of the outer radial maximum, it is suitable in this application since all processes studied here are dominated by large impact parameters and correspondingly large electron-core distances. In the usual manner, the wave function $\Psi(\mathbf{r},\hat{\xi},t)$ is substituted into the time-dependent Schrödinger equation giving rise to coupled first-order differential equations for the coefficients $a_i(t)$. These equations are solved for a large number of impact parameters, subject to initial conditions, and squares of the probability amplitudes $a_i(\infty)$ times the impact parameter are integrated over the impact parameter to obtain cross sections. Convergence of the expansion in Eq. (7) is of course an important concern. It was normally found adequate to include seven PRM functions and a sufficient number of AO's to represent 15 values of n and a selected set of l, m_l substates. For example, the calculations we report for initial state $42s$ (and $J=0$ or 1) were performed using the following basis set: $n=41$, 42, 43 ($l=0$, $m_l=0$, and $1\leq l\leq 5$ with $m_l=0,\pm 1$), $n=40$ ($l=1$ with $m_l=0,\pm 1$, and $1\leq l\leq 5$ with $m_l=0$), $n=44$ ($l=1,2$ with $m_l=0,\pm 1$, and $3\leq l\leq 5$ with $m_l=0$), and similar groupings of final states in near resonance with those expected following $\Delta J=\pm 1$ transitions in the target molecules, i.e., following reactions (2) and (3). The decisions to ignore various l,m_l substates were based in part on trial and error sampling of their contributions to the total cross sec-

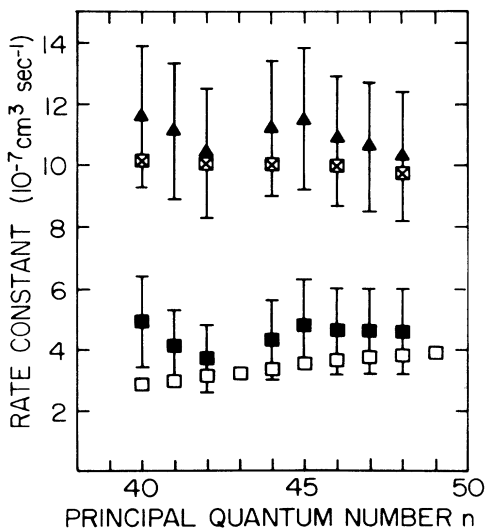

FIG. 2. Rate constants for total collisional depopulation and reaction (1). Experimental results: ⟊, total depopulation; ⟊, reaction (1). Theory-reaction (1): □, semiclassical calculations; ⊠, impulse approximation.

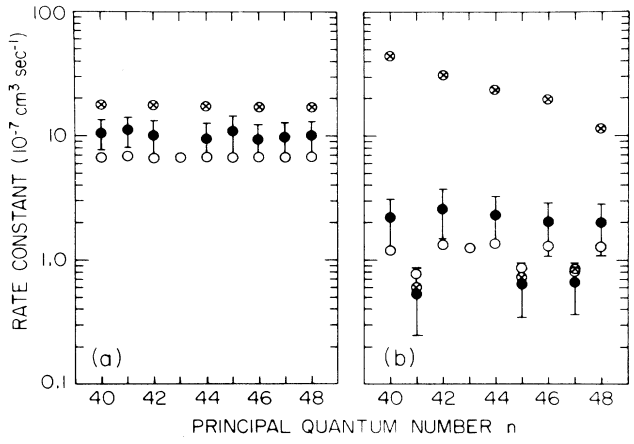

FIG. 3. Rate constants for (a) reaction (2) and (b) reaction (3). Experimental results: ⟊. Theory: ○, semiclassical calculations; ⊗, impulse approximation.

tions. Test calculations also were carried out using a much larger electronic basis set. As the basis set was expanded to include larger values of l and m_l, we observed some tendency toward populating states of larger l and m_l (and thus toward better agreement with the experimental observations which suggest that collisions predominantly populate high-l states). However, although the final l,m_l distribution changed in character, the total cross sections summed over all final l and m_l changed by less than 15% when the larger basis set was used. In all cases, the important states (PRM + AO) were found to be those in near resonance ($\Delta E \sim 0$) with the initial state. The cross sections summed over all final l and m_l presented here are considered to be within 25% of being fully converged. As evident from Figs. 2 and 3, rate constants derived using this theory are in good agreement with the experimental data. Theoretical cross sections for population of specific final l,m_l states are not reported because these results are less well converged. The calculations suggest that in a given J-changing collision, a redistribution among final l and m_l states may occur over a range of atom-molecule separations that extends far beyond the region where the ΔJ interaction is most probable. We are continuing to investigate the dynamical processes that influence the final l and m_l distributions.

The measured rate constants for rotational excitation [reaction (3)] are substantially smaller than those for rotational deexcitation [reaction (2)] and have a much greater variation with n. This results, in part, because the manifolds of excited states available for population by reaction (3) are well separated in energy. The magnitudes of the energy imbalances ΔE associated with transitions from the different initial parent states to the lower-n manifold that represents the best energy match can therefore assume a sizeable range of values, extending from ~ 0.06 to ~ 3.5 cm^{-1}. The measured rate constants for reaction (3) are plotted in Fig. 4 as a function of ΔE. Also included are rate constants obtained using the quantum-mechanical impulse approximation as described by Petitjean and Gounand.[6] As expected, both theory and experiment indicate that the rate constants for reaction (3) decrease as ΔE increases, i.e., as the collision becomes less energy resonant. The observed ΔE dependence is somewhat greater than that suggested by the semiclassical theory but is very much less than that predicted on the basis of the impulse approximation. This is not altogether surprising given the large dipole moment of HF (~ 1.92 Debye) because the strong long-range electron-molecule interaction tends to remove the

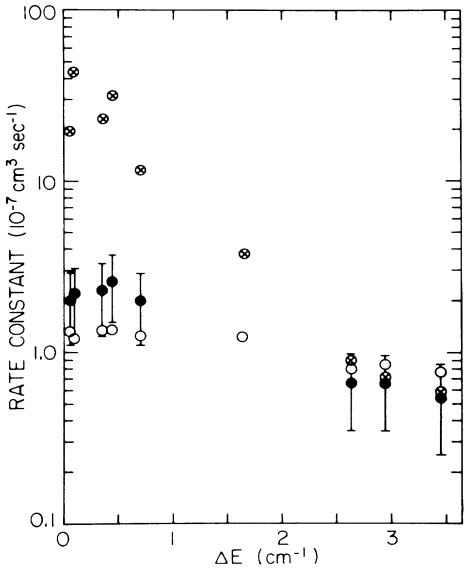

FIG. 4. Rate constants for reaction (3) as a function of the magnitude of the energy imbalance ΔE. Experimental results: ⧳. Theory: ○, semiclassical calculation; ⊗, impulse approximation.

energy degeneracy. This observation is consistent with the findings of Petitjean *et al.*[4] in their study of Rydberg atom collisions with NH_3. It is interesting to note that a number of the energy imbalances associated with reaction (3) are very small, and are comparable to those associated with reaction (2) ($\lesssim 0.4$ cm^{-1}). Even in these cases the measured rate constants for reaction (3) are substantially less than those for reaction (2); the physical reasons for this difference are likely to involve both the densities of final electronic states and the "geometric" properties of both the initial and final electronic states.

The present work again demonstrates the enhancement of n-changing collisions by near energy resonance, and shows that collisions of Rydberg atoms with even strongly polar molecules can be described using a semiclassical theoretical approach.

The research of A.K., L.N.G., K.A.S., and F.B.D. is supported by the National Science Foundation under Grant No. PHY 84-05945 and the Robert A. Welch Foundation. That of M.K. and N.F.L. is supported by the Office of Basic Energy Sciences, Division of Chemical Sciences, U. S. Department of Energy, and the Robert A. Welch Foundation.

*Present address: Argonne National Laboratory, Argonne, IL 60439.

[1]R. F. Stebbings, F. B. Dunning, and C. Higgs, J. Electron Spectrosc. Relat. Phenom. **23**, 333 (1981).

[2]C. Higgs, K. A. Smith, G. B. McMillian, F. B. Dunning, and R. F. Stebbings, J. Phys. B **14**, L285 (1981).

[3]F. G. Kellert, K. A. Smith, R. D. Rundel, F. B. Dunning, and R. F. Stebbings, J. Chem. Phys. **72**, 3179 (1980).

[4]L. Petitjean, F. Gounand, and P. R. Fournier, Phys. Rev. A **33**, 143 (1986); **33**, 1372 (1986).

[5]See also articles by M. Matsuzawa and by A. P. Hickman, R. E. Olson, and J. Pascale, in *Rydberg States of Atoms and Molecules*, edited by R. F. Stebbings and F. B. Dunning (Cambridge University Press, Cambridge, 1983).

[6]L. Petitjean and F. Gounand, Phys. Rev. A **30**, 2946 (1984).
[7]B. G. Zollars, C. Higgs, F. Lu, C. W. Walter, L. G. Gray, K. A. Smith, F. B. Dunning, and R. F. Stebbings, Phys. Rev. A **32**, 3330 (1985).
[8]F. G. Kellert, T. H. Jeys, G. B. McMillian, K. A. Smith, F. B. Dunning, and R. F. Stebbings, Phys. Rev. A **23**, 1127 (1981).
[9]J. W. Farley and W. H. Wing, Phys. Rev. A **23**, 2397 (1981).
[10]M. Matsuzawa, Phys. Rev. A **20**, 860 (1979); **18**, 1396 (1978).
[11]M. R. C. McDowell and J. P. Coleman, *Introduction to the Theory of Ion-Atom Collisions* (North-Holland, Amsterdam, 1970); for an application of semiclassical theory to Rydberg atom collisions with atomic targets see, for example, J. Derouard and M. Lombardi, J. Phys. B **11**, 3875 (1978).
[12]S. Prestoiv and N. F. Lane, Phys. Rev. A **33**, 148 (1986).